# AN INVESTIGATION INTO "RATE OF RISE" DETECTION SYSTEMS FOR DUST EXPLOSION SUPPRESSION

H. N. Phylaktou, C.L. Gardner*, G.E. Andrews, D. Barry**, A. Slattery
Department of Fuel and Energy
School of Process, Environmental and Materials Engineering
The University of Leeds
Leeds, LS2 9JT
Tel. 0113 2332505, fax. 0113 2440572, email. h.n.phylaktou@leeds.ac.uk
*Technology Transfer Associate, Explosion Hazards Ltd / University of Leeds
**Explosion Hazards Ltd, Gate 2 Lymm Marina, Warrington Lane, Lymm, Cheshire
WA13 0SW, Tel 01925 755153, fax.01925 755892

Explosion suppression provides a method for extinguishing a growing fireball and relies on early detection of an incipient explosion. This is most commonly achieved by 'set-point' pressure detection. A disadvantage of this method is the potential of false activation of the suppression system due inherent process pressure fluctuations. An alternative method which might avoid this potential problem is based on 'rate of rise' detection. The objective of this paper is to present the fundamental scientific basis for the appropriate setting and effective operation of 'rate of rise' systems, highlight some of the important variables and problem areas and compare its performance to 'set-point' detection. An explosion model was developed, validated and used to predict the performance of the two detection methods. Analysis of a real example process operation suggested that a rate of rise detector would be independent of both the process mean operating pressure and the magnitude of pressure fluctuations. It was also shown that for the same process and explosion characteristics, the predicted flame ball volume and overpressure at the time of 'rate of rise' detection was significantly lower than that for 'set-point' detection. The lowest performance (although significantly higher than that of the 'set-point') was predicted to be for slow burning explosions, and this should be the determining design condition for 'rate of rise' detection. Additionally, the results suggest the potential of successfully employing suppression systems activated by 'rate of rise' detection in plant equipment previously considered unsuitable for suppression.

Keywords: explosion, dust, rate of rise, detection, suppression

## INTRODUCTION

Potential explosion hazards are to be found throughout industry handling combustible powders/dusts. As a result most countries now have legislation and standards providing guidance for practicable precautions against potential dust explosion hazards and to prescribe safety measures to control their occurrence. Protection measures include containment, inerting, venting and suppression.

For explosion containment the plant must be designed to contain the maximum pressure generated by an explosion [1]. This is normally combined with a system of isolation to prevent explosion transmission from one vessel to another via connecting pipework.

The basis behind the application of inerting as a method of explosion protection is the ability to reduce the oxygen concentration of a dust/air cloud below the minimum required for ignition and so render it inert. Nitrogen, carbon dioxide and flue gases are examples of inert gases used for this method. Inerting is facilitated by a relatively closed process and accurate monitoring of the process oxygen concentration [2].

Most published research has been carried out on venting technology, as traditionally there has been a greater demand for this cheaper type of protection. Explosion venting relies on the relief of overpressure through the opening of appropriately sized and pressure-rated apertures. There is no attempt to control the rate of burning and it is therefore based on the complete burning of the dust cloud and the full growth of the fireball with associated maximum burning rate. Limitations to the application of venting include the ability to discharge vented material in the form of a burning dust cloud, to a safe location. Plants processing toxic dusts which cannot be released to the atmosphere are not suitable for explosion venting.

Explosion suppression involves early detection of the explosion and the rapid discharge of suppressant into the protected volume. Typical suppressants include dry powders, water and fluorinated hydrocarbons. The efficacy of a suppression system depends on a number of parameters including the time period between mixture ignition and suppressant interaction with the expanding flame front (= time for detection, control, actuation and suppressant delivery), the location and number of suppressant containers and mass of suppressant delivered. Guidance for the design of explosion suppression systems is limited and usually proprietary information.

The propagation mechanism of an explosion may be physically or chemically controlled. Heat transfer between dust particles is usually considered to control the propagation rate of dust explosions. Hence in order to suppress most dust explosions it is essential to quench the combustion wave. Discharging a spray of liquid or powder into a growing fireball results in a number of complex effects including quenching (heat abstraction from the combustion zone by energy transfer), free radical scavenging (active species in the suppressant compete with chain-branching reaction necessary for flame propagation), wetting (unburned dust particles are rendered non-flammable by absorption of liquid suppressant) and inerting (concentration of suppressant in suspension renders the unburned mixture inflammable). This latter effect is important for protection against the recognised problem of re-ignition of a post-suppression dust/air atmosphere.

## EXPLOSION DETECTION TECHNOLOGY

### COMMON DEVICES

During the initial stages of flame growth, the speed of the generated pressure wave is that of the speed of sound (nominally 340 m/s), compared to the estimated flame speed of < 10 m/s (for low turbulence conditions). Pressure detection then offers a means of activating a system of suppressant injection into a fireball during the early stages of its growth. The most common method of pressure detection for dust explosion protection involves a static pressure detector, essentially comprising a contact membrane and fixed micro-switch, electrically connected to suppressant containers via a supply and monitoring unit or in more complex systems via a central processing unit. If the pressure level is greater than the detector set-point, the membrane is forced into contact with the fixed micro-switch, closing an electrical circuit resulting in activation of the suppression system. The detector set-point can be adjusted by moving the fixed micro-switch relative to the membrane, or altering the membrane's resistance to bending by varying its thickness.

Optical (IR, UV) flame sensors may be used instead of pressure sensors for detecting the initial explosion. However, consideration has to be given to the fact that explosible dust clouds have high optical densities even at distances of only 0.1m [3]. This limits the ability to sense a small initial flame in a large dust cloud. A more practical application of optical detectors is in advance inerting systems for detecting flames entering ducts between process units, along which dust concentrations are relatively low.

## PROCESS PRESSURE FLUCTUATIONS

By nature, the majority of industrial process plants experience spurious pressure fluctuations due to both process or accidental pressure surges. A simple example might be a gravity-fed hopper into which product is emptied via a catch-gate from an upstream drier. The sudden release of a large volume of material into the hopper could cause an air volume displacement, resulting in a pressure rise. If the pressure level exceeds that of the static detection level, then switching occurs in the detector and the suppression system is fired. In effect, the explosion protection system has been activated without an explosion.

The falsely-activated release of suppressant into a process can result in loss of product, process down-time and re-commissioning of the suppression system. These factors ultimately result in significant cost to the process operators. A more serious result could conceivably be the permanent disarming of the suppression system by the process operators in order to eliminate this cost despite the loss of explosion protection. In order to avoid unwanted suppression system activation, the design of the detector has to be such that system activation can only be triggered by an explosion.

## CURRENT RATE DEVICES/SCOPE FOR ALTERNATIVE

If it can be validated that the rise in pressure due to a process pressure change, $(dP/dt)_{pr}$, is relatively slow compared to the initial rate of pressure rise due to an explosion, $(dP/dt)_{ex}$, then the rate of pressure rise could be used as the determining parameter for explosion detection. The detector would be designed to activate if the system rate of pressure rise was greater than $(dP/dt)_{pr}$. The difference between $(dP/dt)_{pr}$ and $(dP/dt)_{ex}$ gives a 'window' for safe operation of the detector. An accurate knowledge of both $(dP/dt)_{pr}$ and $(dP/dt)_{ex}$ would be needed to apply this theory.

The use of rate of pressure rise as a detection criterion is not a new concept. A number of such detector systems are commercially available, normally in conjunction with a suppressant system. At present, such systems are fairly sophisticated and comparatively expensive, as they are usually made available in conjunction with addressable data logging and processing units. Such systems may be appropriate and cost effective for large (or new) plant systems, but medium and small scale plant owners/operators do not accept that they need this level of sophistication and they find the cost and complexity prohibitive. They would prefer simple, self-contained detection units, designed to operate in relatively harsh process conditions with limited service/calibration requirements.

The technology for such simpler systems is available and a prototype device, developed as part of this project, is currently undergoing field testing and evaluation.

However, it is not our objective here to present the detailed design of this device, but rather to communicate the fundamental scientific basis for the appropriate setting and effective operation of "rate of rise" systems, and highlight some of the important variables and problem areas.

## EXAMPLE OF TYPICAL PROCESS PRESSURE FLUCTUATIONS AND SIGNIFICANCE

The use of a rate of rise detector relies on the rate of increase in system pressure due to a process fluctuation being significantly lower than that generated during the early stages of a dust explosion in that system. In order to investigate this requirement, pressure histories have been recorded for a number of protected systems during normal operation. The different process vessels examined varied in geometry and volume. A commercial transducer was employed with a portable data logging system. A feature of the data acquisition system was the ability to automatically increase the sampling rate (to a maximum of 16 Hz) if the pressure level increased above an operator-specified level. This allowed the recording system to operate continuously for time periods of typically five days. The output from the recording system included the minimum and maximum values of both the absolute system pressure and rate of pressure rise.

This was used as a preliminary method for identifying process equipment where there might be significant pressure fluctuations, and this is followed by much higher resolution monitoring of specific plant over shorter periods of time.

An example of a recorded pressure trace is shown in Fig 1(a). The process vessel essentially comprised of a weigh-hopper (0.895 $m^3$) into which powder was pneumatically fed from a silo via a grinding operation. The maximum overpressure recorded in the hopper was 60 mbar. If the hopper was protected with a suppression system with a nominal static membrane detection pressure of 30 mbar (normally referenced to atmospheric pressure), the system would have been triggered by this process fluctuation on four occasions in the 9 hour period shown.

It might be suggested that an increase in the detector set-point to, say, 70 mbar would eliminate spurious operation. This might be balanced with an increase in system protection by for example increasing the amount and storage pressure of the suppressant (larger and faster delivery). However, (although not shown on Fig 1(a) – see Figure caption) the recorded pressure dropped below atmospheric to a minimum of –170 mbar. If ignition occurred at this pressure, a positive explosion pressure change of 240 mbar would be generated before detection. The fireball volume developed at the time of detection may then be large enough to negate the ability of the triggered suppression system to limit the final explosion pressure to a safe design level. It should be noted that referencing the pressure detector to the process pressure is not an option as this would result in the system never triggering. Referencing to absolute vacuum might be an option (although not for this example) if it can be assured that the process operating pressure is fixed.

It is clear therefore that a set-point activated suppression system would not be suitable for this example system or for numerous other systems operating under similar conditions.

The maximum recorded rate of pressure rise, $(dP/dt)_{pr}$ was 180 mbar/s (not shown on Fig 1(b) – see Figure caption). If it could be validated that the rate of pressure rise during the early stages of an explosion, $(dP/dt)_{ex}$ was greater than 180 mbar/s at the time of detection, then the application of a ‘rate of rise’ detector might be possible. A more detailed analysis of this system will be presented later.

## THE RELEVANCE OF $K_{ST}$ METHODOLOGY

ISO standards [4] describe the measurement of explosion indices for dust/air mixtures such as maximum explosion pressure, rate of pressure rise and $K_{st}$, given by,

$$K_{st} = \left(\frac{dP}{dt}\right)_{max} V^{1/3} \qquad (1)$$

where $(dP/dt)_{max}$ is the maximum rate of pressure rise (bar/s) and V is the test vessel volume ($m^3$).

An important feature of suppression technology is the rapid detection and extinguishment of the explosion fireball at an early stage of its development. At this early stage, the flame radius is small compared to the vessel radius and $(dP/dt)_{ex}$ is relatively slow compared to the maximum pressure rise, $(dP/dt)_{max}$ that would be reached if the explosion was allowed to develop further and the flame radius was comparable to that of the vessel. It is clear therefore that values of $(dP/dt)_{max}$ reported in the literature are not applicable to the present problem.

The $K_{st}$ and $(dP/dt)_{max}$ methodology has been developed for and is mainly used for the design of explosion venting systems. $K_{st}$ and $(dP/dt)_{max}$ data are strictly not applicable to dust explosion suppression design, where activation should occur when the flameball volume is small and $(dP/dt)_{ex}$ is substantially smaller than $(dP/dt)_{max}$.

## A TIME DEPENDENT EXPLOSION MODEL

For a detailed evaluation of $(dP/dt)_{ex}$ during the initial stages of flame growth, an explosion model was developed based on ideal gas state equations. The model is based on calculating the flame area for a given mass of mixture burnt and using the resultant burnt volume to compute the change in system pressure. A time-step process is used to calculate the pressure rise. Rate of pressure rise, fireball volume and radius are then computed and the magnitude of these parameters at a given pressure (eg detection) can be calculated. The influence of vessel volume and mixture burning velocity (and of other parameters) can be investigated.

### MODEL ASSUMPTIONS

The key assumptions in the model are as follows:

a. both the reactants and products are assumed to be in the gas state
b. the gas/dust/air mixture is uniformly mixed, and contained within a rigid spherical vessel of radius $R_V$, such that its volume is equal to the volume under consideration,
c. at time $t_0$ combustion is initiated at the centre of the vessel by a small spherical flame front of defined radius $R_{f,0}$ (of the order of 2 to 5 mm),
d. combustion takes place within a very thin flame front which delineated the boundary between the burnt and unburnt mixtures,
e. all molecular species (reactants and products) obey the perfect gas law,
f. burnt gases attain uniform flame temperature within negligible time,
g. the flame front propagates radially from the point of ignition, at a propagation rate much smaller than the velocity of sound,
h. therefore, the pressure could be taken as uniform throughout the vessel,
i. the burnt and unburnt gas temperature and density are uniform within the two distinct regions,
j. the unburnt gas is compressed isentropically ahead of the expanding flame front,
k. the process is adiabatic,
l. the laminar burning velocity is assumed to be constant throughout the combustion process,
m. natural convection effects, such as buoyancy, are negligible.

The progress of the explosion is charted in small time steps of 1 ms or the time required for combustion of 1/150$^{th}$ of the mixture mass (whichever is smallest). This method gives a higher resolution when the rate of burning is fast (e.g. towards the final stages of the explosion when the flame area is large or when the turbulence is high resulting in a high burning velocity). During each time step combustion of a fraction of the mixture takes place. The burnt mass is added to the previously burnt amount. Combustion at each step is assumed to take place at constant volume, but the effect of the burnt and unburnt region isentropic expansion and compression are taken into account in calculating the energy content of each region and in calculating the resulting conditions at the end of each time step.

## GOVERNING EQUATIONS

It is best to consider such equations as they apply at an arbitrary $i^{th}$ timestep of the calculation procedure. Since the system is closed, then the total mass within the system remains constant and equal to that at time zero ($m_0$), i.e. before combustion begins. At any time i during the explosion

$$m_i = m_{b,i} + m_{u,i} = m_0 \qquad (2)$$

The subscripts b and u refer to the burnt and unburnt state respectively. The fraction of mass burnt during the $i^{th}$ step was given by:

$$(dm_b)_i = A_{f,(i-1)}\, \rho_{u,(i-1)}\, S_L\, \beta\, dt \qquad (3)$$

where dt is the time interval, $A_f$ is the flame area, $\rho_u$ is the unburnt gas density, $S_L$ is the laminar burning velocity of the mixture (discussed later) and $\beta$ is the turbulence factor, defined as the ratio of turbulent (actual) to laminar burning velocity. $\rho_u$ and $A_f$ are used in this calculation at the $i^{th}$ time-step with the values assigned to them at the end of the previous (i-1) step. For this reason it is important that the time-step chosen is not too large in order to avoid any significant errors due to the discontinuity necessarily imposed by the time-step procedure.

From consideration of the ideal gas laws and bearing in mind that the volume V of the system remains constant and equal to ($V_u + V_b$) at all times, it can be shown that the pressure P at the end of time-step i is given by:

$$P_i = R\left(T_{b,i} n_b + T_{u,i} n_u\right)/V \qquad (4)$$

where, R is the universal gas constant, T is the temperature and n is the number of moles (given by the mass divided by the mean molecular weight).

The unburnt gas temperature can determined from the isentropic compression equation:

$$T_{u,i} = T_{u,(i-1)}\left(P_i/P_{i-1}\right)^{\left(\gamma_{u,(i-1)}-1\right)/\gamma_{u,(i-1)}} \qquad (5)$$

where $\gamma$ is the specific heat ratio of the unburnt gas (taken as constant at 1.4)

Once the temperatures $T_b$ & $T_u$ , the pressure P and the mass of burnt and unburnt gas, $m_b$ & $m_u$ were calculated at the end of the $i^{th}$ iterative loop, then the volume of the burnt gas could be calculated and assuming a spherical flame shape then the flame area $A_f$ could be derived along with the other quantities that are required in Eq. 3 to initiate the next iterative time step.

It should be noted that although the laminar burning velocity, $S_L$, is assumed to be constant, it is in fact dependent on the temperature and pressure [5].

## COMMENTS ON THE SUITABILITY OF A GAS BASED MODEL FOR DUST EXPLOSIONS

The dusts most likely to fit a gas-based explosion model are those of natural and synthetic organic materials which would emit appreciable amounts of volatile gases when heated. Additionally, the volatilisation process must be fast enough so that volatilisation is not the rate determining step and this, in general, would imply small particle sizes (large surface to volume ratio) [6].

Two critical characteristic parameters used in the model are the laminar burning velocity, $S_L$, and the burnt gas temperature, $T_b$. For spherical flame propagation in a closed vessel these two parameters effectively determine the rate of burning, the rate of pressure rise and the maximum pressure. Comparability of these parameters for gas and dust/air mixtures would suggest that a similar modelling approach could be justified.

A number of experimental studies aimed at measuring $S_L$, for various dust/air mixtures have been reported. Apparatus employed have included burners [7,8], tubes [8-11,] and constant volume bomb methods [12-15]. A recent European research project, CREDIT, has been undertaken [16] in order to estimate laminar burning velocities of a variety of dusts (the Company partner was a co-sponsor of this project). Vertical tubes into which dust was gravity fed were used and the cloud ignited by a low energy spark. The base of the tube was open to atmosphere so that burnt gas was free to expand behind the flame resulting in its propagation velocity to be its characteristic burning velocity. Typical values reported are listed in Table 1. A feature of the reported results was a considerable data scatter and confidence in assigning a value to $S_L$ for a specific dust/concentration would be limited. Also shown in Table 1 are measured and calculated adiabatic flame temperatures [10]. With regard to the flame temperatures the deficit between the calculated and measured values was attributed to radiative heat losses.

| DUST | **Conc. ($g/m^3$)** | **$S_L$ (m/s)** [16] | **$T_b$ (K) (at stoich.)** [10] | |
|---|---|---|---|---|
| | | | **Meas.** | **Calc.** |
| Lycopodium | 60-175 | 0.23-0.41 | ~1600 | 2213 |
| Cornstarch | 80-200 | 0.31-0.59 | 1573 | 2193 |
| Maize starch | 45-300 | 0.36-0.55 | | |
| Lignite dust | 420-640 | 0.34-0.47 | - | - |
| Silicon | 150->500 | 0.43-0.89 | - | - |

Table 1. Laminar burning velocities and flame temperature measurements and calculations for dust/air mixtures.

The dust/air data reported in Table 1 is comparable to literature values for gas/air mixtures. For example for hydrocarbon gases, say stoichiometric methane to heptane /air mixtures, typical values of $S_L$ range from 0.35 to 0.55 m/s while adiabatic flame temperatures are of the order of 2200K. On the basis of the comparability of these properties and of others such as minimum ignition energies, Bradley and Lee [6] argued that fine-organic-dust combustion is similar to gas burning.

## MODEL VALIDATION

The ability of the computer model to accurately predict an explosion development was tested against two sets of experimental data of stoichiometric methane/air explosions in spherical or near spherical, totally enclosed vessels. The model could not be tested against experimental dust explosion data as no such data (presented in sufficient detail) could be found in the literature.

The first set of data was extracted from a report by Garforth [17]. The apparatus used was an 80 mm radius sphere with experimental measurements taken from a continuous photographic record of the flame front position and a transient recording of the pressure development.

In Figs. 2(a) and 2 (b) these experimental measurements (shown as symbols) are compared with the results of the present computational simulation (solid lines). In general the agreement between experiment and prediction was excellent for both flame growth and pressure history.

The second set of experimental data was obtained in this laboratory [18] in a cylindrical vessel, 0.5 m in diameter and 0.5 m long. A transducer recorded the pressure development, while a radial array of 14 thermocouples was used to record the time of flame arrival. It should be noted that this vessel was significantly larger than that of Garforth [17] and it was not spherical. In the computer simulation, a spherical vessel was assumed of equal volume to the experimental cylinder.

Figure 3(a) compares the experimental record of the flame radius development with the computational prediction. The simulated flame propagation was in very good agreement with the experimental data except for the last fifth of the total flame travel, where some disagreement was noted. The pressure signal comparison in Fig. 3(b) showed a similar pattern. Excellent accord was achieved between the predicted and the recorded pressure up to about 100 ms into the explosion. From Fig. 3(a) it can be seen that this corresponded to the flame being less than 50 mm from the vessel wall. At this point the model began to underestimate the system pressure until the very last stages of the combustion when the prediction overestimated the measured pressure.

A possible explanation for the small discrepancies between the model and the experiment could be provided by consideration of the differences between the actual flame shape and that assumed in the model. In an explosion the flame propagation speed is dependent on the burning velocity and on the induced unburnt gas velocity ahead of the flame. At the walls of a vessel the gas velocity has to be zero, and therefore as the walls are approached the gas flow velocity is decelerated and so is the corresponding part of the flame front. In a non-spherical vessel, the expansive forces behind the flame are directed towards parts of the front that are still away from walls resulting thus in a higher propagation rate of these flame sections. This mechanism leads to deformation of the flame shape which in the final stages of the explosion takes the approximate form of the confining geometry. This difference in flame shape results in differences in the flame area and thus in the combustion rate. The flame area in the experimental study was at its maximum just before it reached the vessel walls and was larger than that of the corresponding theoretical flame. This resulted in the model underestimating the combustion rate which translated into lower predicted pressure levels in the system as shown in Fig. 3(b). When the experimental flame arrived at the vessel walls parts of it were quenched, while combustion continued into the corners of the enclosure. The loss of flame area was also accompanied with large heat transfer outside the system because of the contact of the hot combustion products with the cold vessel walls. This resulted in the reduction of the rate of pressure increase in the vessel as shown by the pressure record in Fig. 3(b). These phenomena were not accounted for in the theoretical model, and in fact at this time the theoretical flame was at its maximum size, and therefore the rate of pressure increase was at its maximum. This resulted in the predicted pressure exceeding the experimental measurements as shown. Overall, however, the differences between this second set of experimental data and the model predictions were small and the agreement was good.

From the findings of this limited validation exercise it could be concluded that the theoretical model could be used with some confidence to predict pressure development and flame movement in stoichiometric methane/air explosions (or for similarly behaving gas and dust/air mixtures in near spherical vessels with central ignition. Further validation is required, particularly for a range of dust/air mixtures.

## EXAMPLE MODEL PREDICTIONS AND DISCUSSION

GENERAL

Figure 4 is an example simulation of full explosion development in a 5m$^3$ vessel handling a combustible mixture with a burning velocity of 0.4 m/s and a burnt gas (flame) temperature of 2230K. The flame radius ratio, $R_f/R_v$ (flame radius divided by the vessel radius), the overpressure ratio ($\Delta P/\Delta P_{max}$) and the rate of pressure rise (dP/dt) are plotted against time. It should be clarified that the overpressure ratio is defined relative to the initial vessel pressure $P_o$ (rather than the ambient pressure) according to

$$\frac{\Delta P}{\Delta P_{max}} = \frac{P - P_o}{P_{max} - P_o} \tag{6}$$

where P is the pressure in the system at any time during the explosion and $P_{max}$ is the maximum adiabatic pressure reached at the end of the explosion (typically 8-9 bara for stoichiometric hydrocarbon/air mixtures).

Figure 4 shows that there is no significant overpressure (compared to the maximum) or rate of pressure rise for a relatively long period of time. For example, before the first 5% rise in pressure, approximately 300 ms have elapsed (almost 50% of the total explosion duration). While this is a beneficial feature as it allows time for the explosion protection system to react, the flame radius curve shows that at 300 ms, the flame radius has reached almost 80% of the vessel radius, i.e. the flameball size is probably too large to be effectively suppressed.

The flameball size is a very important parameter in the design of a suppression system as it determines the required amount and rate of delivery of suppressant. In general, the volume of injected suppressant should be significantly greater than that of the flameball. This effectively means suppressant interaction with the flame when it is still relatively small (of the order of less than 0.5m diameter for most practical volumes).

The overpressure ratio and rate of pressure rise are shown as a function of the flame radius ratio in Fig. 5. For most practical systems (unless specifically designed to withstand high pressures) the set-point suppression activation pressure is of the order of 10-50 mbar, corresponding to an overpressure range of less than 0.6% of the maximum explosion overpressure.

A zoomed-in view of this overpressure range is shown in the inset on Fig. 5. A typical set-point activation pressure of 30 mbaro is also marked on this graph. It can be seen that this overpressure corresponds to a flame radius of approximately 30% of the vessel radius (corresponding to a flame diameter of about 0.6m) or a volume ratio (flame to vessel) of about 2.7%. It should be noted that these values are not specific to this vessel and in fact the overpressure ratio dependence on the flame radius ratio is a universal relationship, and largely independent of actual vessel volume and mixture burning properties.

A detailed knowledge of the process operating pressure profile is critical to the successful design and operation of a set-point detection system. Process pressure fluctuations, operating pressures under partial vacuum conditions and even variable atmospheric pressures may cause false activation of the suppression system, or ineffective suppression if the flame-ball is allowed to grow too large. Under these circumstances, ‘rate of rise’ detection may be the only appropriate solution. These matters are discussed in detail below with reference to the example system introduced earlier.

## EXAMPLE APPLICATION TO A SPECIFIC SYSTEM

For the example weigh-hopper process described earlier, the operating pressure range was –170 to +60 mbarg, and the fastest rate of pressure rise, $(dP/dt)_{pr}$ was 180 mbar/s. The volume of the vessel was 0.895 m$^3$ ($R_v$ = 0.598m). The material handled was starch (with a typically reported laminar burning velocity in the range 0.2-0.5 m/s and adiabatic flame temperature in the range of 1500 to 2000K [10, 16]. There is no quantitative data on the actual turbulence levels in the vessel and for the purposes of this illustration, two turbulence factors, $\beta$, are used (1 and 3), indicating no turbulence and a moderate turbulence level respectively. The explosion model was run for the different conditions listed in Table 2, approximately encompassing the range of process operating conditions.

Two criteria for activating a suppression system were examined. The first was a set detection pressure of +70 mbar above atmospheric (to avoid spurious activation) and the second was based on a 'rate of rise' of 360 mbar/s, which was twice the maximum process rise, $(dP/dt)_{pr}$. This is a higher tolerance margin with regard to operating conditions, compared to a factor of 1.2 (70/60) for the set-point system. This higher tolerance is obviously an advantage with respect to avoidance of spurious system activation and the validity of using a higher tolerance margin will be justified by the results as there is no reduction in operational performance.

Effectively four sets of operating conditions were considered; high and low process pressure, $P_o$ (1 and 0.8 bara), and fast and slow mixture burning rate, defining the realistic extremes of the operating/explosion conditions.

Considering the 1 bara initial pressure and fast burning explosion (higher $S_L$, $T_b$ and $\beta$) it can be seen from Table 2 that the 'set-point' detector would activate the suppression system when the overpressure is 70 mbar and the rate of pressure rise is 886 mbar/s. Conversely, the 'rate of rise' detector would activate the suppression system on the rate of pressure rise reaching 360 mbar/s, when the overpressure is just 1 mbar. This corresponds to a much smaller flame (as indicated by the flame radius and volume ratios). By comparison, the flame volume at the time of 'set-point' detection is approximately 80 times larger than for the 'rate of rise' detector.

This situation becomes worse with the 'set-point' detector when the process pressure, $P_o$ is 0.8 bara at the time of initiation of the explosion. In this case the pressure has to increase by 270 mbar before 'set-point' detection[#]. This condition makes no operational difference to the 'rate of rise' detector, as shown. The flame volume ratio for the two detectors for this scenario is now approximately 240.

This difference in flame volume at the time of detection has significant implications on the effectiveness of a suppression system as discussed earlier. In the example system, a suppression system activated by a 'rate of rise' detector would be far more likely to successfully extinguish the flame.

For the slow burning scenario in Table 2, the operational ability of the 'rate of rise' detector is reduced somewhat with the flame volumes being approximately 25 times larger than for the faster burning conditions and with the overpressures at the time of detection, $P_{det}$, being about 20 mbar. Nevertheless these values still demonstrate a significant performance advantage of the 'rate of rise' detector over the 'set-point' detector.

---

[#] This problem could not be rectified by the use of absolute pressure instead of gauge pressure detection, because the process pressure is not constant.

| Process conditions | | Mixture burn. characteristics | | Static 'set-point' detector $P_{set}$ = 70 mbar* | | | | 'Rate of rise' detector $(dP/dt)_{ex} = 2 \times (dP/dt)_{pr}$ | | | |
|---|---|---|---|---|---|---|---|---|---|---|---|
| $P_o$ bara | β | $S_L$ m/s | $T_b$ K | **$\Delta P_{det}$ mbar** | dP/dt mbar/s | $R_f/R_v$ | $V_f/V_v$ | $\Delta P_{det}$ mbar | **dP/dt mbar/s** | $R_f/R_v$ | $V_f/V_v$ |
| 1 | 3 | 0.5 | 2200 | **70** | 9210 | 0.381 | 0.055 | 1 | **360** | 0.089 | 0.0007 |
| 0.8 | 3 | 0.5 | 2200 | **270** | 21251 | 0.604 | 0.220 | 1 | **360** | 0.097 | 0.0009 |
| 1 | 1 | 0.2 | 1500 | **70** | 886 | 0.390 | 0.059 | 18 | **360** | 0.251 | 0.016 |
| 0.8 | 1 | 0.2 | 1500 | **270** | 1947 | 0.619 | 0.237 | 20 | **360** | 0.284 | 0.023 |
| 0.8 | 1 | 0.2 | 1500 | | | | | 57 | **720**** | 0.391 | 0.059 |

*relative to atmospheric (1bara)
** $(dP/dt)_{ex} = 4 \times (dP/dt)_{pr}$

Table 2 Comparative assessment of set-point and 'rate of rise' detection for different process conditions and mixture burning characteristics.

It might not be immediately obvious why in a slow burning explosion the overpressure and the flameball volume should be significantly larger than for a fast burning explosion, for the same rate of pressure rise. To understand the mechanism of this behaviour it must be appreciated that dP/dt is proportional to the rate of mass burning $dm_b/dt$. From Eq. (3),

$$\frac{dP}{dt} \propto \frac{dm_b}{dt} \propto \beta S_L A_f \tag{7}$$

for the fast explosion β and $S_L$ are higher than for the slow explosion and therefore for this case the same dP/dt can only be reached when the flame area, $A_f$ is larger than that of the fast explosion. A larger flame area means a larger flame volume which in turn means a larger fraction of the total mass has been burned, and hence a higher corresponding overpressure has been generated (although this may be somewhat compensated for by the lower flame temperatures of the slow explosion).

These results additionally demonstrate that a system based on a 'rate of rise' detector should be designed to cope with slow burning mixtures, rather than fast ones. This is a very important finding as it is opposite to the intuitive worst-case scenario.

As the results in Table 2 show, a fast explosion (resulting form high laminar burning velocity or high turbulence levels) will be detected very early in its development when the overpressure and flameball volume are both very small.

It should be noted that the volume of 0.895 $m^3$ of the example system discussed above is close to that considered as unsuitable for explosion suppression, due to the speed of explosion development in these volumes. The results in Table 2 show that the method of 'rate of rise' could provide a much earlier detection than traditional set-point method, and therefore allow more time for suppressant delivery. The fireball volume would also be much smaller and therefore the effectiveness of the suppressant will be increased.

Additionally, the 'rate of rise' based suppression system could potentially be used to protect equipment that would normally be designed to contain an explosion, (such as grinders/milling equipment), as these items have previously been considered unsuitable for suppression. The potential of extinguishing ie stop explosion here and so prevent transmission to connected vessels.

## CONCLUSIONS

Dust handling equipment requiring explosion protection can often be characterised by process pressure fluctuations which can result in inadvertent activation of suppression systems which rely on 'set-point' detection technology.

An explosion model has been developed and used to compare the performance of 'set-point' and 'rate of rise' detection for an example system operating under a fluctuating pressure range from partial vacuum to slightly over atmospheric.

Analysis of an example process system showed that,

- A 'set-point' detector set at a pressure level marginally above the maximum recorded process pressure (so as to avoid false activation) would activate when the flame volume is relatively large. This situation was significantly worsened when the pressure at which the model explosion was initiated was a partial vacuum.
- The 'set-point' detector was largely insensitive to the mixture burning characteristics
- A 'rate of rise' detector set to activate on the rate of pressure rise reaching twice the maximum process rate of pressure change was predicted to activate much earlier in the explosion when the pressure and flame volume were one or two orders of magnitude smaller than the corresponding 'set-point' results.
- This has important benefits in the design of appropriate suppression systems and provides higher confidence in the effectiveness of such systems since they could activate when the flame is small.
- The performance of a 'rate of rise' detector was insensitive to the process operating pressure range.
- The more severe the explosion development the better was the performance of a 'rate of rise' detector.
- The lowest performance (although significantly higher than that of the 'set-point') was predicted to be for slow burning explosions, and this should be the determining design condition for 'rate of rise' detection.
- Additionally, the results suggest the potential of successfully employing suppression systems activated by 'rate of rise' detection in plant equipment previously considered unsuitable for suppression, and instead designed to withstand full explosion pressures

For a more comprehensive confirmation of the above conclusions, the explosion model needs to be validated against dust explosion tests. To this end, experimentally determined laminar burning velocities of dust/air mixtures are required, as well as knowledge of realistic turbulence factors in typical plant.

The successful application of 'rate of rise' detection requires highly resolved process rate of pressure change data for specific systems.

## ACKNOWLEDGEMENTS

We thank the Teaching Company Directorate for co-sponsoring this research through TCS Programme No.: 264801

**REFERENCES**

1. Schofield, C., A Guide to Dust Explosion Prevention and Protection, Part 1-Venting, IChemE, 1984.
2. Ten Cate, M., Inerting and Flushing Technologies: Critical Observations, Europex - 3rd World Wide Seminar on the Explosion Phenomenon and on the Application of Explosion Protection Techniques in Practice, 1999.
3. Eckhoff, R.K., Dust Explosions in the Process Industries, Butterworth-Heinemann, 1991.
4. ISO, 6184/1, 1985.
5. Epstein, M., Hauser, G.M., Tilley, B.J., Bannon, Jr., C.H., Wise, L.S., Thistleton, P, Harper, R.L., Couture, M.J. and Blair, B.R, A computer model for the estimation of peak pressure for sonic, vented tetrafluoroethylene decompositions., J. Loss., Prev. Process Ind., 3., p.370, 1990.
6. Bradley D., and Lee, J.H.S, On the mechanism of propagation of dust flames, 1st Int. Coll. on Expl. of Ind. Dusts, p.220, 1984
7. Mazurkiewicz, J. and Jorosinski, J., Investigations of a Laminar Cornstarch Dust-Air Flame Front, Proceedings of the 6th International Colloquium on Dust Explosions, 1993.
8. Van der Wel, P., Ignition and Propagation of Dust Explosions, PhD Thesis, 1993
9. Proust, C. and Veysiere, B., Fundamental Properties of Flames Propagating in Starch Dust-air Mixtures, Combustion Science and technology, 62, 1988
10. Proust, C., Experimental Determination of the Maximum Flame Temperatures and of the Laminar Burning Velocities for some Combustible Dust-air Mixtures, Proceedings of the 5th International Colloquium on Dust Explosions, 1993.
11. Mazurkiewicz, J., Jorosinski, J. and Wolanski, P., Investigations of Burning Properties of Cornstarch Dust-Air Flames, Grain Dust Explosions and Control, 1993.
12. Tezok, F.I., Kauffman, C.W., Sichel, M. and Nicholls, J.A., Turbulent Burning Velocity Measurements for Dust/Air Mixtures in a Constant Volume Spherical Bomb, Progress in Astronautics and Aeronautics, 105, 1986.
13. Bradley, D., Chen, Z. and Swithenbank, J.R., Burning Rates in Turbulent Fine Dust-Air Explosions, 22nd Symposium (International) on Combustion, The Combustion Institute, 1988.
14. Tai, C.S., Kauffman, C.W. and Sichel, M. et al, Turbulent Dust Combustion in a Jet-Stirred Reactor, Progress in Astronautics and Aeronautics, 113, 1988.
15. Kauffman, C.W., Srinath, S.R., Tezok, F.I., Nicholls, J.A. and Sichel, M., Turbulent and Accelerating Dust Flames, 20th Symposium (International) on Combustion, The Combustion Institute, 1984.
16. Pedersen, L.S. and Van Windergen, K., Measurement of Fundamental Burning Velocity of Dust-Air Mixtures in Industrial Situations, CMR-95-F20018, 1995.
17. Garforth, A.M., The Spherical Bomb Method for Laminar Burning Velocity Determination; Experimental Results and Critical Appraisal, Report No. 75, University of Witwatersand, Johannesburg, 1977.
18. Phylaktou, H.P., Gas Explosions in Long Closed Vessels with Obstacles, PhD Thesis, University of Leeds, 1993.

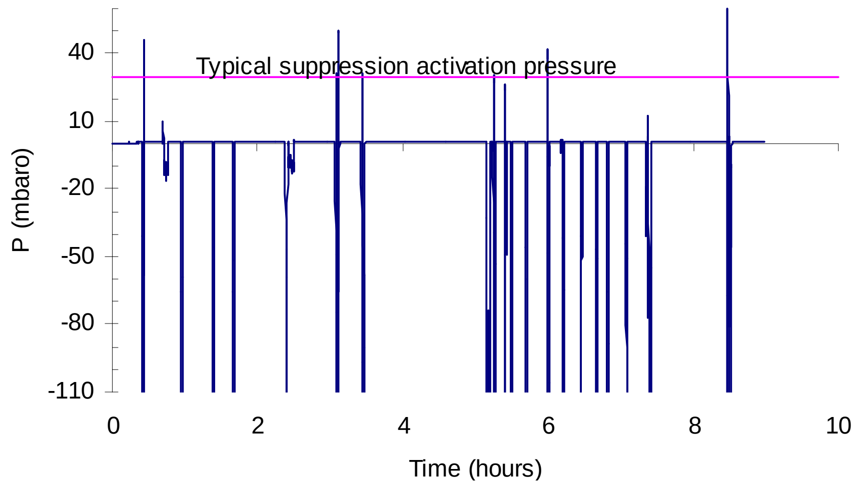


(a)

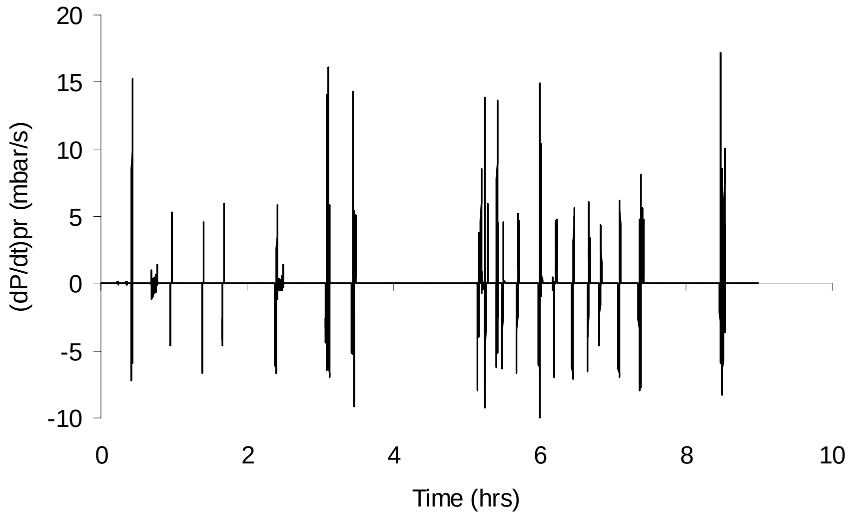


(b)

Figure 1. Example of (a) process pressure fluctuations and (b) corresponding rate of pressure rise in a weigh-hopper (0.895 $m^3$) into which powder is pneumatically fed from a silo via a grinding operation. (*Note: the actual maxima and minima in the above charts have been truncated because of sample reduction during transfer form the data logger to the graphics package. The actual values of maxima and minima are as quoted in the text)*

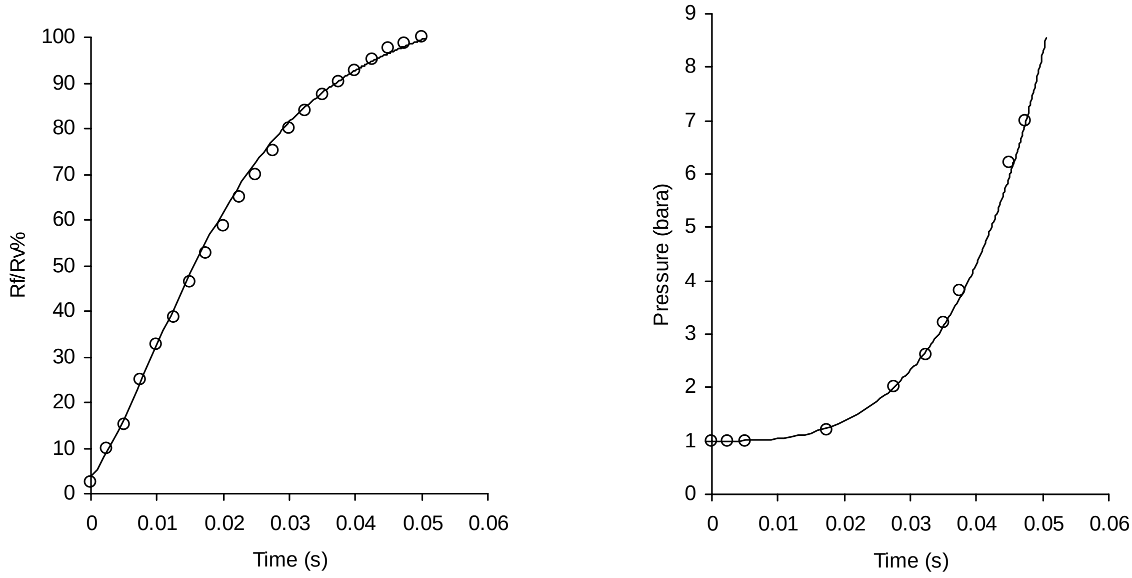


(a) (b)

Figure 2. Comparison of experimental data (symbols) from Ref. [17] with model predictions (solid lines) ($S_L$=0.40 m/s). (a) Flame radius as a percentage of vessel radius, (b) Absolute pressure

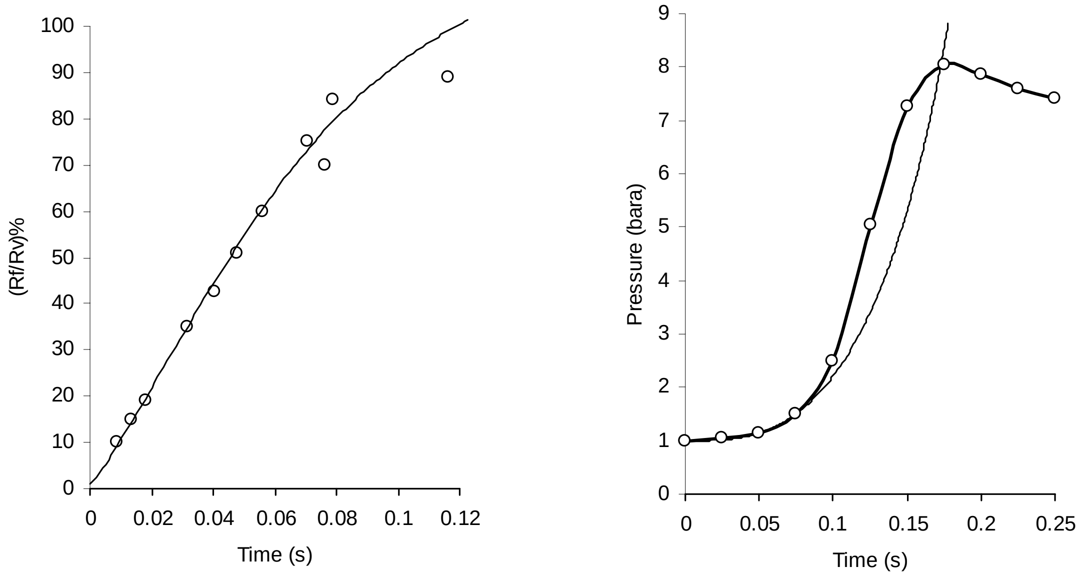


(a) (b)

Figure 3. Comparison of experimental data (symbols) from Ref. [18] with model predictions (solid thin lines) ($S_L$=0.40  m/s). (a) Flame radius as a percentage of vessel radius, (b) Absolute pressure

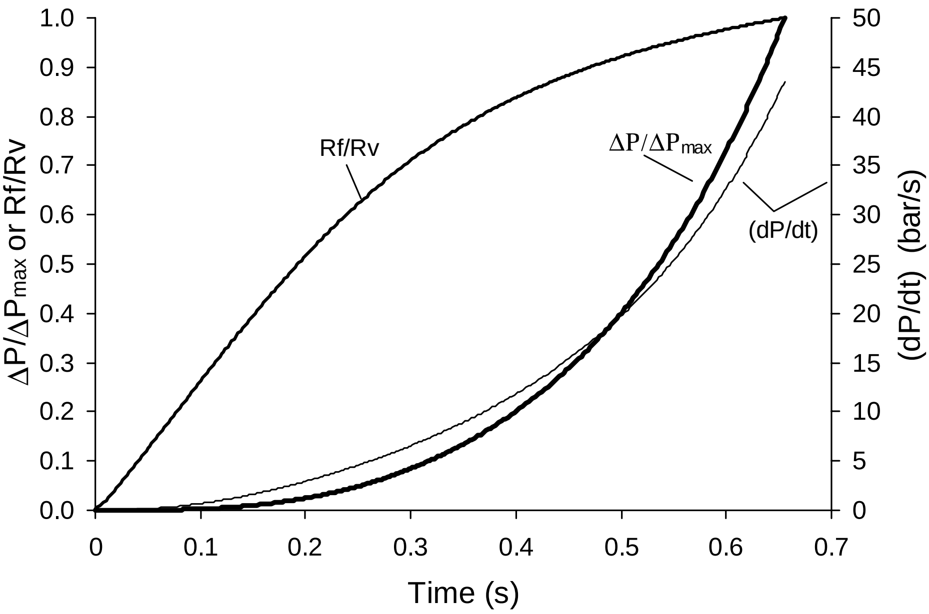


Figure 4. Predicted variation of dimensionless overpressure and flame radius, as well as of the rate of pressure rise, with time for an explosion in a closed 5 m$^3$ vessel. (Mixture $S_L$=0.4 m/s, $T_b$=2230)

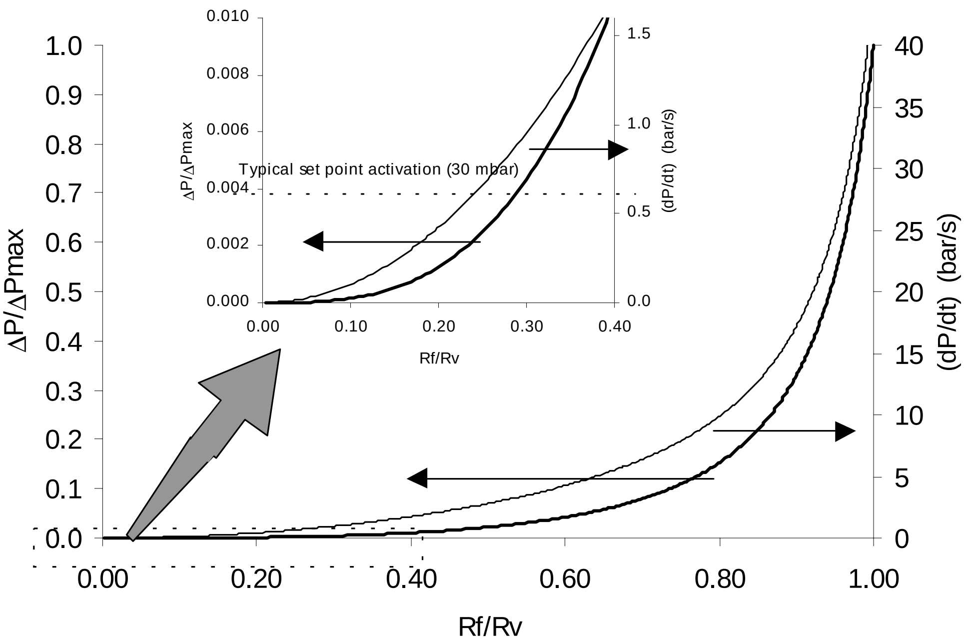


Figure 5. Predicted rate of pressure rise and dimensionless overpressure as function of dimensionless flame radius, for an explosion in a closed 5 m$^3$ vessel. (Mixture $S_L$=0.4 m/s, $T_b$=2230K). The inset is a zoomed-in view of the region of explosion detection systems for suppression activation.